



Cite this: *Dalton Trans.*, 2024, **53**, 15032

Received 6th August 2024,  
Accepted 7th August 2024  
DOI: 10.1039/d4dt02248c  
[rsc.li/dalton](http://rsc.li/dalton)

## Accessing five- and seven-membered phosphorus-based heterocycles via cycloaddition reactions of azaphosphines†

Ethan D. E. Calder, Louise Male and Andrew R. Jupp \*  
Ethan D. E. Calder, Louise Male and Andrew R. Jupp

Heterocycles containing both phosphorus and nitrogen have seen increasing use in recent years in luminescent materials, coordination chemistry and as building blocks for inorganic polymers, yet their chemistry is currently dominated by five- and six-membered derivatives. Seven-membered P/N heterocycles are comparatively scarce and lack general, high yielding syntheses. Here, we explore the synthesis and characterisation of 1,2,5-diazaphosphepines from azaphosphines. The mechanism has been probed in detail with both computational and experimental studies supporting a stepwise mechanism to form a five-membered ring, and subsequent ring expansion to the diazaphosphepine. Regioselective synthesis of five- and seven-membered rings is possible using asymmetric alkynes. The Lewis acidic borane  $B(C_6F_5)_3$  could either catalyse the formation of the seven-membered ring ( $^iPr$  derivative) or trap out a key intermediate via a frustrated Lewis pair (FLP) mechanism ( $^iBu$  derivative).

## Introduction

The incorporation of phosphorus into heterocyclic systems can lead to significant changes in their properties and reactivity. Phospholes, first synthesised in 1959,<sup>1</sup> have emerged as highly valuable compounds in numerous fields ranging from photochemical applications to coordination chemistry, and often display aromaticity.<sup>2–5</sup> Utilising phosphorus alongside its lighter group 15 congener, nitrogen, can bestow further reactivity in the heterocycle, particularly when featuring a direct  $P^V=N$  bond. This arises due to the highly polarised nature of the  $P^V=N$  bond, which yields significant single-bond character and a more basic nitrogen centre. Such phosphorus and nitrogen containing heterocycles have subsequently been used in areas including luminescent materials<sup>6</sup> and as building blocks for inorganic polymers.<sup>7</sup>

The majority of currently reported phosphorus/nitrogen containing heterocycles are based on either five- or six-membered rings.<sup>8</sup> Seven-membered rings containing both phosphorus and nitrogen and comparatively scarce. The most common approach for preparing seven-membered P/N rings relies on the condensation of amines with halophosphine

derivatives, with concomitant release of HCl, which necessarily affords products with direct P–N bonds.<sup>9–11</sup> There are fewer examples of P/N heterocycles that contain solely P–C bonds, yet heterocycles of this type recently have been applied as ligands for Ni in electrocatalysts or as chelating ligands for lanthanide ions,<sup>12–14</sup> and in medicinal applications (Fig. 1A).<sup>15</sup> Azaphosphepines are unsaturated seven-membered P/N heterocycles, and convenient and high-yielding synthetic routes to such heterocycles remain limited in scope. The most pertinent examples of azaphosphepine synthesis for this current study are ring-expansions *via* P–N cleavage of an appropriate five-membered ring precursor. In 1990, Ried *et al.* reported the ring-expansion of a five- to seven-membered ring *via* the cleavage of a P–N bond with electronically activated alkynes.<sup>16</sup> The products were characterised crystallographically and spectroscopically, although the mechanism of reaction was not discussed. In 2019, Lozovskiy *et al.* also reported intramolecular ring-expansion by P–N bond cleavage in a five-membered ring to yield a seven-membered ring.<sup>17</sup> The only prior example of 1,2,5-diazaphosphepine chalcogenides was reported by Barkallah *et al.*, where 2,2'-(phenylphosphoryl)bis(cyclopentan-1-one) (or the sulfur and selenium analogues) was reacted with hydrazine and acetic acid (Fig. 1B), although the products were not structurally characterised.<sup>18</sup>

Azaphosphines are phosphorus-containing analogues of triazenes with the chemical formula  $ArN=N-PR_2$ , with a trivalent phosphorus centre that can be exploited for further reactivity. A limited range of azaphosphines were synthesised in the 1970s and 1980s, but no further reactivity was

School of Chemistry, University of Birmingham, Edgbaston, Birmingham, B15 2TT, UK. E-mail: [a.jupp@bham.ac.uk](mailto:a.jupp@bham.ac.uk)

† Electronic supplementary information (ESI) available. CCDC 2356185 (6), 2356186 (4), 2356187 (10), 2356188 (8), 2356189 (9), 2356190 (7), 2356191 (11) and 2356192 (7-BCF). For ESI and crystallographic data in CIF or other electronic format see DOI: <https://doi.org/10.1039/d4dt02248c>



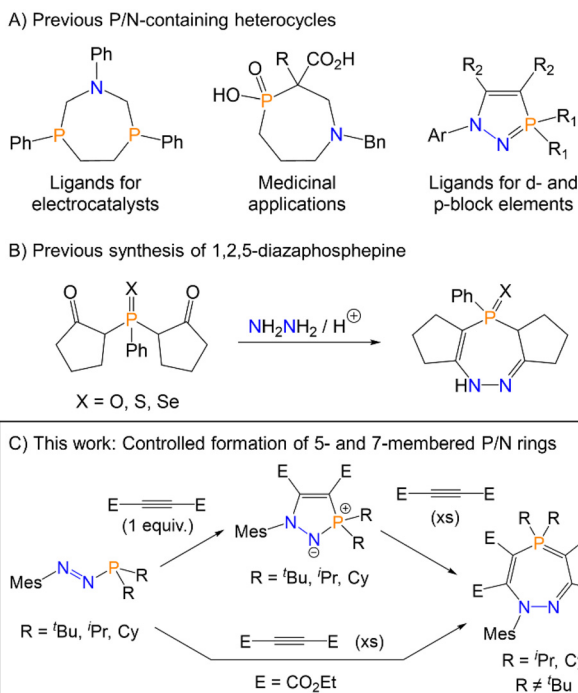


Fig. 1 (A) Applications of previously reported P/N-containing heterocycles. (B) Only previous example of a 1,2,5-diazaphosphepine. (C) This work.

explored.<sup>19–21</sup> This class of compounds was ignored until 2021, when Cummins and co-workers synthesised  $\text{MesN}_2\text{PA}$  ( $\text{Mes} = \text{mesityl}$ ,  $\text{A} = \text{anthracene}$ ).<sup>22</sup> This molecule was shown to undergo a range of cycloaddition reactions with unsaturated substrates, including  $[\text{Na}(\text{dioxane})_{2.5}][\text{PCO}]$  and  $\text{AdCP}$  ( $\text{Ad} = \text{adamantyl}$ ), with loss of the labile anthracene moiety. The following year, the same group isolated azophosphines of the form  $\text{ArN}_2\text{PR}_2$  ( $\text{R} = \text{iPr, Cy, Ph, NMe}_2$ ), and demonstrated the cycloaddition reactions of these species with cyclooctyne, which yielded five-membered N-heterocyclic iminophosphoranes.<sup>23</sup> One example of a 1,3-dipolar cycloaddition of the azophosphine ( $p\text{-MeC}_6\text{H}_4\text{N}_2\text{PPH}_2$ ) with the electronically activated alkyne dimethyl acetylenedicarboxylate ( $\text{C}(\text{CO}_2\text{Me})_2$ ) was also reported. Very recently, we reported a general synthetic route to azophosphines which allowed for tolerance of bulky  $P$ -substituents, and demonstrated the use of these systems as ligands in  $\text{Ru}$  complexes *via* the phosphorus and nitrogen centres.<sup>24</sup>

Motivated by these results, we reasoned that azophosphines may be able to serve as precursors to a wider range of phosphorus and nitrogen containing heterocycles beyond those currently reported. In this manuscript, we report the synthesis and characterisation of five- and seven-membered phosphorus- and nitrogen-containing rings from azophosphines. The seven-membered rings are the first crystallographically characterised 1,2,5-diazaphosphepines, and the mechanism of this transformation has been probed both computationally and experimentally. The interactions of these species with the

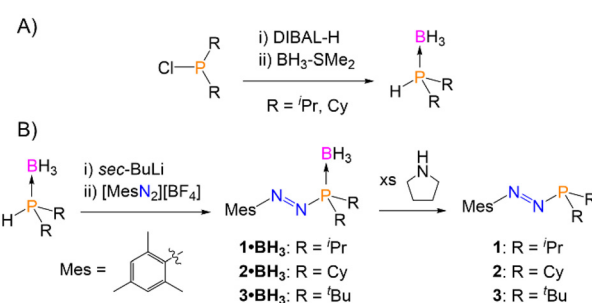
Lewis acidic borane  $\text{B}(\text{C}_6\text{F}_5)_3$  has also been explored, which was shown to catalyse the formation of the seven-membered heterocycle for the  $\text{iPr}$ -derivative and result in the trapping of a key intermediate for the  $\text{iBu}$ -derivative.

## Results & discussion

### Synthesis and characterisation of heterocycles

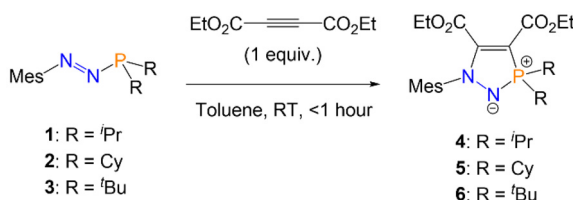
We recently reported a new synthesis of azophosphines *via* the reaction of arenediazonium salts ( $[\text{ArN}_2][\text{BF}_4]$ ;  $\text{Ar} = \text{Mes}$  or  $(p\text{-NMe}_2\text{C}_6\text{H}_4)$ ) with deprotonated secondary phosphine-boranes ( $\text{HPR}_2\cdot\text{BH}_3$ ), although the  $P$ -substituent was limited to  $\text{R} = \text{iBu}$  and  $\text{Ph}$ .<sup>24</sup> The same synthetic procedure was used here, and was shown to tolerate smaller alkyl  $P$ -substituents. The secondary phosphine-boranes  $\text{HPR}_2\cdot\text{BH}_3$  ( $\text{R} = \text{iPr, Cy}$  (cyclohexyl)) were synthesised from the corresponding dialkylchlorophosphines by a modified literature procedure (Scheme 1A).<sup>25</sup> Deprotonation of these substrates with *sec*-BuLi at  $-78\text{ }^\circ\text{C}$ , followed by reaction with mesitylenediazonium tetrafluoroborate ( $[\text{MesN}_2][\text{BF}_4]$ ) allowed for the formation of the target azophosphine-boranes ( $\text{MesN}_2\text{PR}_2\cdot\text{BH}_3$ ) **1**–**3** ( $\text{R} = \text{iPr}$ ) and **2**–**3** ( $\text{R} = \text{Cy}$ ) as a purple oil or purple solid, respectively, in moderate yields following purification (**1**–**3** = 41%, **2**–**3** = 44%; Scheme 1B). The borane protecting group could then be fully removed *via* reaction with pyrrolidine to yield the free azophosphines ( $\text{MesN}_2\text{PR}_2$ ) **1** ( $\text{R} = \text{iPr}$ ) and **2** ( $\text{R} = \text{Cy}$ ) in good yields (**1** = 78%, **2** = 71%; Scheme 1), both as red oils.

With azophosphines **1** and **2** in hand, as well as the previously reported azophosphine **3** ( $\text{MesN}_2\text{P}(\text{iBu})_2$ ), we next investigated the cycloaddition reactions of these systems. No reactivity was observed with the  $\text{C}\equiv\text{C}$  bond of diphenylacetylene, nor the  $\text{C}\equiv\text{N}$  bond of benzonitrile. However, the reaction of azophosphines **1**–**3** with one equivalent of the electron-poor alkyne diethyl acetylenedicarboxylate ( $\text{C}(\text{CO}_2\text{Et})_2$ ) in toluene gave an immediate colour change from red (**1**, **2**) or purple (**3**) to pale yellow, and formation of the five-membered heterocycles ( $\text{R} = \text{iPr}$  (**4**),  $\text{Cy}$  (**5**),  $\text{iBu}$  (**6**); Scheme 2). Reaction monitoring by  $^{31}\text{P}\{^1\text{H}\}$  NMR spectroscopy showed quantitative conversion from azophosphine to product; removal of the solvent *in vacuo* yielded analytically pure compounds **4**–**6** in good isolated yields (80–85%).



Scheme 1 (A) Synthesis of phosphine-borane precursors. (B) Synthesis of azophosphine-boranes and free azophosphines.





**Scheme 2** Synthesis of five-membered heterocycles **4–6** via azophosphines.

Single crystals of **4** were grown by slow evaporation of a hexane solution, and of **6** by slow evaporation of a THF-hexane solution (1:10, v/v), allowing for characterisation of the solid state structures by single-crystal X-ray diffraction (SXRD) (Fig. 2A and B). Both **4** and **6** possess planar five-membered cores, as shown in the side-on views in Fig. 2C and D. **6** displays an N–N bond length of 1.4115(19) Å, indicative of an N=N single bond,<sup>26</sup> and significantly elongated compared to the N=N double bond [1.226(6) Å] observed in the previously reported solid state structure for its azophosphine-borane precursor **3**·BH<sub>3</sub>.<sup>24</sup> The P–N bond length of **6** exists somewhere between a single and double bond [1.6461(14) Å], but clearly shortened compared to the P–N bond of **3**·BH<sub>3</sub> [1.769(5) Å]. **4** displays similar N–N [1.4096(17) Å] and N–P [1.6442(14) Å]

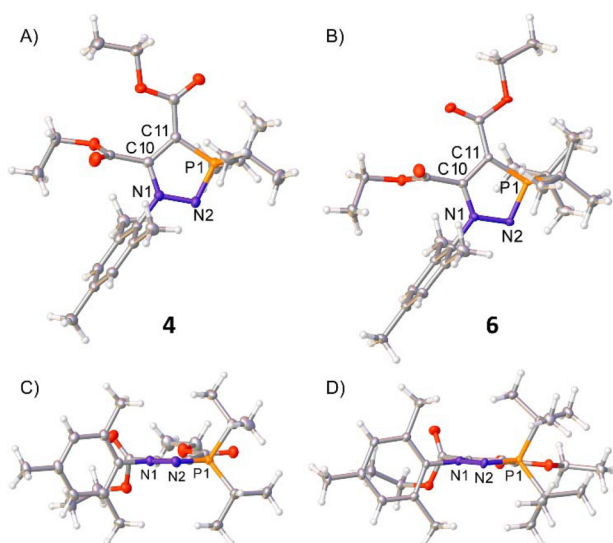
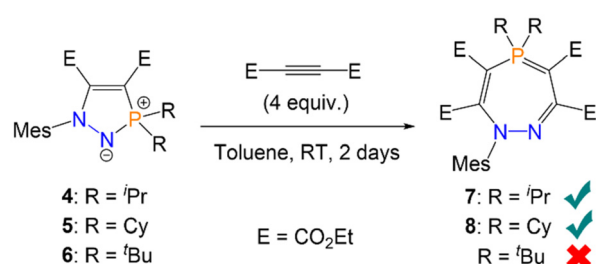


**Fig. 2** Single crystal structures of **4** and **6**. Top-down view shown in (A) and (B); side-on view for (C) and (D). Selected bond distances (Å) and torsion angles (°): **4**: N1–N2 1.4096(17), N2–P1 1.6442(14), C10–C11 1.403(2), N1–C1 1.442(2), P1–C18 1.8326(16), P1–C21 1.8244(17), C10–C12 1.503(2), C11–C13 1.436(2), N1–N2–P1–C11 –2.37(11), N1–C10–C11–P1 –0.34(17); **6**: N1–N2 1.4115(19), N2–P1 1.6461(14), C10–C11 1.401(2), N1–C1 1.442(2), P1–C18 1.8670(18), P1–C22 1.8655(17), C10–C12 1.503(2), C11–C13 1.437(2), N1–N2–P1–C11 –5.77(11), N1–C10–C11–P1 –2.50(18). **4** crystallised with two product molecules in the asymmetric unit; only one is shown here for clarity and bond metrics are statistically similar for both independent molecules so only one set is given above. Thermal ellipsoids were drawn at the 50% probability level at 100 K.<sup>27</sup>

bond lengths to **6**. The planarity and bond lengths of both **4** and **6** are in good agreement with the N-heterocyclic iminophosphoranes reported by Cummins, which also displayed planar heterocyclic cores and comparable N–N and P–N bond distances.<sup>23</sup> To corroborate these findings, density functional theory (DFT) and natural bond orbital (NBO) analyses were carried out (see ESI† for details). The optimised structures are in good agreement with the observed solid-state structures, with similarly planar heterocyclic cores and N–N and P–N bond metrics. Natural population analysis (NPA) showed a highly electron-rich N2 nitrogen centre (–0.859 for **4**, –0.874 for **6**) and electron-deficient phosphorus centre (+1.809 for **4**, +1.841 for **6**), with calculated Wiberg bond indices for the P–N bonds of 1.07 (**4**) and 1.05 (**6**). These data are suggestive of more single bond than double bond character in the P–N bond.

Given the partial single-bond character of the P–N bond in five-membered rings **4–6**, we hypothesised that this bond could be cleaved by certain substrates to yield larger phosphorus-containing heterocycles, by analogy with the aforementioned ring expansion chemistry.<sup>16,17</sup> Reactions of a P–N bond within five-membered rings has previously been reported with ketones, ketenes, and isocyanates, although in all cases either acyclic or bicyclic structures were observed instead of ring expansion.<sup>28–30</sup> Cummins also reported one example of P–N bond cleavage in an N-heterocyclic iminophosphorane with Ph<sub>3</sub>SiH, although this resulted in loss of the heterocyclic structure and formation of a Ph<sub>3</sub>Si–N(R)–H moiety.<sup>23</sup> Five-membered heterocycle **4** (R = iPr) was thus reacted with an excess (4 equiv.; Scheme 3) of (C(CO<sub>2</sub>Et))<sub>2</sub> in toluene. Monitoring by <sup>31</sup>P{<sup>1</sup>H} NMR spectroscopy showed a new species forming, product **7**, with quantitative conversion within 48 hours at room temperature; the solution also became a visibly brighter yellow colour. **7** could also be formed directly from azophosphine **1**, by reacting **1** with the same excess of (C(CO<sub>2</sub>Et))<sub>2</sub>. Monitoring this latter reaction by <sup>31</sup>P{<sup>1</sup>H} NMR spectroscopy showed **4** initially forming at 74.9 ppm, before giving way to **7** at 60.4 ppm. Analogous reactivity was observed with azophosphine **2** (Mes<sub>2</sub>N<sub>2</sub>PCy<sub>2</sub>), which yielded seven-membered heterocycle **8** via **5**. Recrystallisation and removal of the solvent *in vacuo* yielded analytically pure compounds **7** and **8** in excellent isolated yields (**7** = 88%, **8** = 92%), with no further work-up



**Scheme 3** Synthesis of seven-membered heterocycles **7** and **8** via azophosphines. **6** does not react with excess alkyne to form the analogous seven-membered ring.



necessary. However, when the sterically more hindered azophosphine **3** ( $\text{MesN}_2\text{P}^t\text{Bu}_2$ ) was used, no seven-membered ring could be detected by  $^{31}\text{P}\{^1\text{H}\}$  NMR spectroscopy. Even with a large excess of alkyne (10 equiv.) and heating to 60 °C, only formation of five-membered ring **6** was observed (Scheme 3); heating above 60 °C gave an intractable mixture of products.

Single crystals of **7** and **8** were produced by slow diffusion of *n*-hexane into a concentrated THF solution of the product at −35 °C, for which single-crystal X-ray diffraction revealed the unusual seven-membered ring structure featuring cleavage of the P–N bond by a second equivalent of alkyne (Fig. 3). In contrast to the planar geometries of five-membered rings **4** and **6**, the seven-membered rings of **7** and **8** feature non-planar, puckered cores (Fig. 3C and D). An analysis of the bond metrics shows that four major resonance structures can be considered for these seven-membered rings ( $\alpha$ ,  $\beta$ ,  $\gamma$ , and  $\delta$  in Fig. 3E). The metric data for **7** and **8** are analogous and so **7** will be discussed here as a representative example. The P1–C13 bond [1.7465(14) Å] is significantly shorter than P1–C11 [1.7851(14) Å], highlighting the contribution from resonance  $\alpha$ . The negative charge in  $\beta$  can also be delocalised into the proximal ester group as shown in  $\gamma$  [C13–C17 = 1.4316(19) Å, C17–O7 = 1.2235(18) Å], or onto N2 as shown in  $\delta$  [C12–C13 =

1.438(2) Å]. The crystallographic data are corroborated by density functional theory (DFT) and natural bond orbital (NBO) analyses (see ESI† for details) for **7**.

### Mechanistic insight

To determine the minimum energy pathway for the formation of five-membered rings **4** and **6**, DFT calculations were carried out (see ESI† for details), using the xylyl group instead of mesityl for the calculations as a simplified model. A recent computational study by Zhang and Su exploring the cycloaddition of structurally related azophosphines with cyclooctyne found a concerted reaction pathway, with an activation barrier of 22.0 kcal mol<sup>−1</sup>.<sup>31</sup> Cummins also calculated the reaction of their  $\text{MesN}_2\text{PA}$  unit with cyclooctyne to be thermodynamically favourable *via* a concerted pathway, with subsequent loss of the anthracene unit.<sup>22</sup> Our calculations showed a stepwise mechanism to instead be preferred for the cycloadditions of azophosphines **1** and **3** with diethyl acetylenedicarboxylate (Scheme 4). Focusing on the pathway for **3** to **6**, initial attack of the phosphorus lone pair (HOMO) of **3** to the alkyne yields the zwitterionic intermediate **I1**, with a corresponding activation barrier of 20.4 kcal mol<sup>−1</sup> (**TS1**) corresponding to P–C bond formation. **I1** adopts a partially allenic, partially bent structure (Scheme 4). This is supported by a C1–C2 bond length of 1.329 Å, consistent with a C=C double bond, and an elongated C2–C3 bond length of 1.401 Å, with a C1–C2–C3 bond angle of 138.3°. The HOMO of **I1** has contributions from both the electron-rich carbon and oxygen centres, while the LUMO is mainly centred on the N=N  $\pi^*$  orbital. Subsequent HOMO to LUMO ring-closing proceeds over a small activation barrier of 3.3 kcal mol<sup>−1</sup> (**TS2**). Product **6** is favoured by 50.1 kcal mol<sup>−1</sup> relative to the starting materials. An identical pathway was

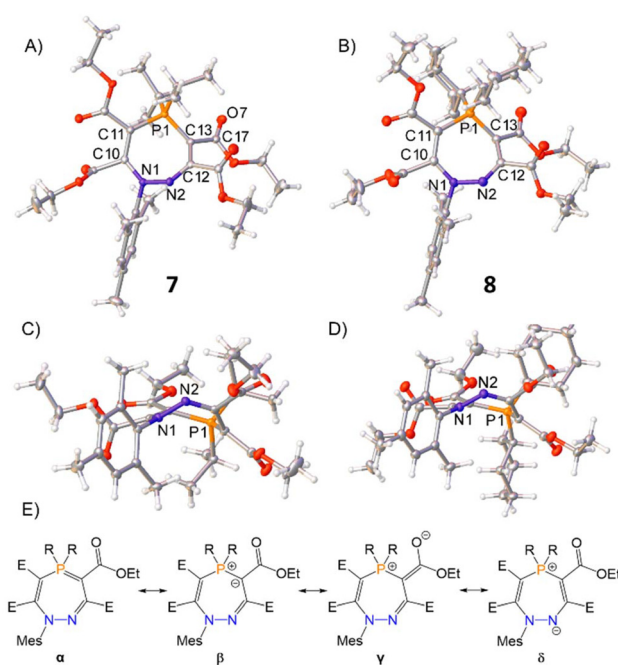
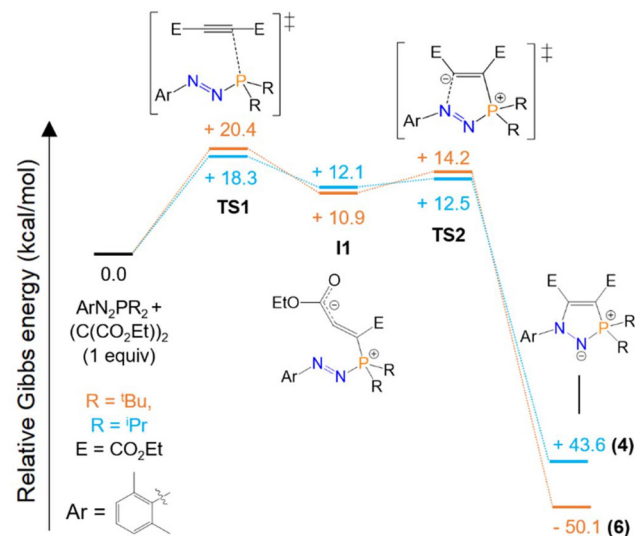


**Fig. 3** Single crystal structures of **7** and **8**. Top-down view shown in (A) and (B); side-on view for (C) and (D). Selected bond distances (Å): **7** N1–N2 1.4172(16), N2–C12 1.2908(18), C12–C13 1.438(2), C13–P1 1.7465(14), C11–P1 1.7851(14), N1–C1 1.4472(17), C10–C14 1.5364(18), C11–C15 1.4659(19), C12–C16 1.5321(19), C13–C17 1.4313(19), P1–C26 1.8381(14), P1–C29 1.8344(14); **8** N1–N2 1.4177(18), N2–C12 1.2926(19), C12–C13 1.443(2); C13–P1 1.7407(16), C11–P1 1.7892(15), N1–C1 1.4487(18), C10–C14 1.531(2), C11–C15 1.480(2), C12–C16 1.530(2), C13–C17 1.434(2), P1–C26 1.8239(14), P1–C32 1.8321(15). Thermal ellipsoids were drawn at the 50% probability level at 100 K.<sup>27</sup> (E) Possible resonance structures for seven-membered heterocycles **7** and **8** (E = CO<sub>2</sub>Et).



**Scheme 4** Computed pathways (Gibbs free energy, kcal mol<sup>−1</sup>) for the cycloadditions of **1** and **3** with  $(\text{C}(\text{CO}_2\text{Et})_2$  to form **4** and **6** at the  $\omega\text{B97XD/def2TZVP//}\omega\text{B97XD(toluene)/def2QZVP}$  level of theory using the xylyl group instead of mesityl for a slightly simplified model. For full computational details see ESI.†

found for the formation of **4** from azophosphine **1**, with similar activation barriers calculated. The preference for a stepwise pathway in our system compared to the previously computed concerted pathways may be rationalised by the stabilisation of the zwitterionic intermediate **I1** by the electron-withdrawing ester groups, and the fact that our study is on *P,P*-dialkyl azophosphines that are more nucleophilic than the previously studied *P,P*-diphenyl systems.<sup>22,31</sup> A preference for stepwise over concerted reaction pathways has previously been shown for cycloaddition reactions of the analogous alkyne dimethyl acetylenedicarboxylate with dienylisobenzofurans.<sup>32</sup>

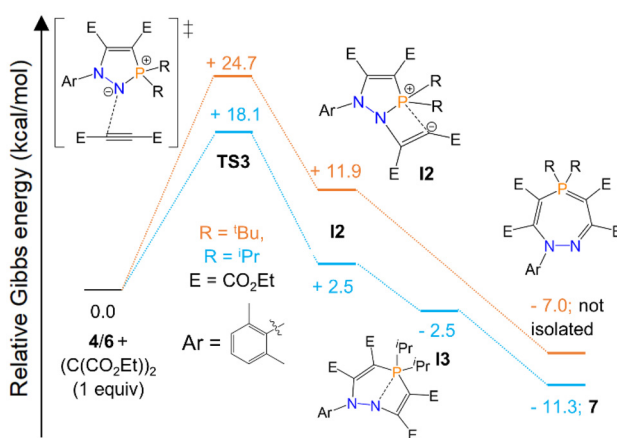
We also sought to determine the minimum energy pathway for the formation of seven-membered ring **7**, and rationalise the why the analogous heterocycle with  $R = {^t\text{Bu}}$  substituents did not form. Our calculations suggest that the first step, corresponding to nucleophilic attack by the dicoordinate nitrogen centre of **4/6** to the alkyne (**TS3**), is the rate-limiting step of the reaction (Scheme 5). This proceeds over an energy barrier of 18.1 kcal mol<sup>-1</sup> for **4** ( $R = {^i\text{Pr}}$ ), but the corresponding energy barrier for **6** ( $R = {^t\text{Bu}}$ ) is significantly higher, at 24.7 kcal mol<sup>-1</sup>. This barrier is accessible for **4** at room temperature, but was inaccessible for **6** in our experiments. Attempts to overcome this barrier by heating the reaction led to an intractable mixture of products. Seven-membered rings **7** and **8** form at room temperature but decompose above 50 °C, which may indicate that if the energy barrier for  $R = {^t\text{Bu}}$  substituents can be overcome at elevated temperatures, the product subsequently decomposes and cannot be isolated. After this first step, the subsequent intermediate, **I2**, adopts a partially allenic and partially bent structure (analogous to **I1**, Scheme 4), although in this case the bent structure is stabilised to a greater extent as the carbanion has a weak interaction with the proximal electron-poor phosphorus centre. We were also able to locate a further intermediate (**I3**), which was only present for  $R = {^i\text{Pr}}$  substituents, in which the P–N interatomic

distance is significantly longer (2.145 in **I3** vs. 1.756 in **I2**) and P–C bond shorter (1.842 in **I3** vs. 2.012 in **I2**). After extensive searching, we were unable to locate any transition states between **I2** and the products, although relaxed potential energy surface scans indicated that these steps would be  $<5$  kcal mol<sup>-1</sup> for  $R = {^i\text{Pr}}$  and  $<7$  kcal mol<sup>-1</sup> for  $R = {^t\text{Bu}}$  and are thus clearly not rate-limiting (see ESI† for further details).

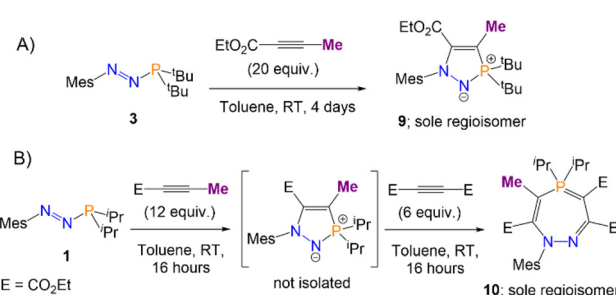
### Regioselective formation of heterocycles

The stabilisation of **I1** (Scheme 4) by electron delocalisation into the ester group prompted us to probe the regioselectivity of these reactions; namely, whether the use of an asymmetric alkyne would yield one, or several, regioisomers. Azophosphine **3** ( $\text{MesN}_2\text{P}^i\text{Bu}_2$ ), was thus reacted with an excess (20 equiv.) of ethyl 2-butynoate ( $\text{H}_3\text{CC}\equiv\text{C}(\text{CO}_2\text{Et})$ ) in toluene. After 4 days, only one major product was observed by <sup>31</sup>P{<sup>1</sup>H} NMR spectroscopy, which after work-up was observed to be product **9** (Scheme 6A). This regioisomer could be confirmed in solution by 2D-NOESY NMR spectroscopy, as a nOe (nuclear Overhauser effect) could be observed between the  ${^t\text{Bu}}$  groups and the methyl protons bound to the ring ( $-\text{C}=\text{CCH}_3$ ), but not between the  ${^t\text{Bu}}$  groups and any of the protons on the ester groups. Single crystals of **9** were grown *via* slow evaporation of a concentrated hexane solution, and SXRD confirmed the product as the expected regioisomer (Fig. 4A). The bond metric data for **9** are similar to those previously discussed for **4** and **6**.

The analogous reaction with azophosphine **1** ( $\text{MesN}_2\text{P}^i\text{Pr}_2$ ) was attempted, as the smaller *P*-substituents could potentially enable access to the corresponding seven-membered ring. Azophosphine **1** was reacted with an excess (12 equiv.) of ethyl 2-butynoate overnight in toluene (Scheme 6B). Complete consumption of the azophosphine was observed by <sup>31</sup>P{<sup>1</sup>H} NMR spectroscopy, and formation of a new species at 72.4 ppm, consistent with formation of a five-membered heterocycle, although we were unable to cleanly isolate this species. There was no evidence of any formation of the seven-membered ring, despite the excess of the alkyne used, which we postulate is due to the reduced electrophilicity of ethyl 2-butynoate compared to diethyl acetylenedicarboxylate (*i.e.* the analogous barrier that would correspond to **TS3** from Scheme 5 in this system is too high to be accessible). However, subsequent addition of an excess (6 equiv.) of the more reactive diethyl



**Scheme 5** Computed pathways (Gibbs free energy, kcal mol<sup>-1</sup>) for the reaction of **4** and **6** with  $(\text{C}(\text{CO}_2\text{Et}))_2$  at the  $\omega\text{B97XD}/\text{def2TZVP}/\omega\text{B97XD}$  (toluene)// $\text{def2QZVP}$  level of theory using the xyl group instead of mesityl for a slightly simplified model. For full computational details see ESI†.



**Scheme 6** Regioselective synthesis of heterocycles **9** (A) and **10** (B) *via* the reaction of azophosphines with ethyl 2-butynoate.



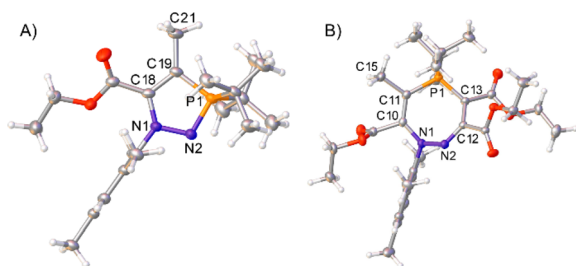


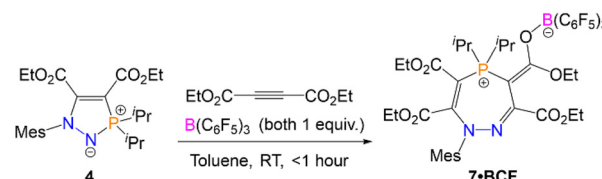
**Fig. 4** Single crystal structures of **9** (A) and **10** (B). Selected bond distances (Å): **9** N1–N2 1.4117(18), N2–P1 1.6382(13), C18–C19 1.390(2), N1–C1 1.4349(18), P1–C10 1.8790(17), P1–C14 1.8618(18), C18–C20 1.485(2), C19–C21 1.508(2), **10** N1–N2 1.4103(18), N2–C12 1.286(2), C12–C13 1.452(2), C13–P1 1.7268(17), C11–P1 1.7737(17), N1–C1 1.444(2), C10–C14 1.519(2), C11–C15 1.529(2), C12–C16 1.526(2), C13–C17 1.430(2), P1–C24 1.8264(18), P1–C27 1.8316(17). **9** crystallised with two product molecules in the asymmetric unit; only one is shown here for clarity. Thermal ellipsoids were drawn at the 50% probability level at 100 K for **9**, and 120 K for **10**.<sup>27</sup>

acetylenedicarboxylate ( $(\text{C}(\text{CO}_2\text{Et}))_2$ ) to this compound yielded species **10** as the sole product. Single crystals of **10** were grown *via* slow evaporation of a hexane solution, for which SXRD confirmed the product as the expected regiosomer of the seven-membered ring (Fig. 4B); this structural assignment was again supported by 2D-NOESY NMR spectroscopy. The formation of products **9** and **10** demonstrate the regioselective synthesis of five- and seven-membered rings from azaphosphines.

### Catalysis and trapping of intermediate

The formation of the seven-membered rings is relatively sluggish, and an excess of the alkyne was often used to drive the reaction to completion in a reasonable timeframe (four equivalents of alkyne required to form **7** in two days). Although the alkyne is relatively volatile and can be recycled for future experiments, we sought to improve the efficiency of the reaction. The rate-determining step for the formation of the seven-membered ring from the five-membered precursor is the attack of the electrophilic alkyne by the nitrogen centre (**TS3** in Scheme 5). We therefore rationalised that a Lewis acidic borane could bind to the alkyne and activate it (thereby lowering the energy of **TS3**), with the caveat that the borane would have to be sterically bulky enough to preclude binding to the nucleophilic nitrogen centre on the five-membered ring and quenching its reactivity. We opted to use tris(pentafluorophenyl)borane (**BCF**),  $\text{B}(\text{C}_6\text{F}_5)_3$ , which is highly Lewis acidic and relatively bulky, and is widely employed as a main-group Lewis acid catalyst and as a component of frustrated Lewis pair catalysts.<sup>33–39</sup>

Five-membered heterocycle **4** ( $\text{R} = \text{Pr}^i$ ) was thus combined with one equivalent of  $(\text{C}(\text{CO}_2\text{Et}))_2$  and one equivalent of  $\text{B}(\text{C}_6\text{F}_5)_3$  in toluene (Scheme 7). The reaction resulted in the rapid formation ( $<1$  hour) of **7-BCF**, in which  $\text{B}(\text{C}_6\text{F}_5)_3$  is bound to an ester group in the corresponding seven-membered ring **7**. This adduct was characterised by SXRD (Fig. 5A) and multinuclear NMR spectroscopy, with **7-BCF** having a



**Scheme 7** Synthesis of **7-BCF** via the reaction of **4** with  $(\text{C}(\text{CO}_2\text{Et}))_2$  and  $\text{B}(\text{C}_6\text{F}_5)_3$ .

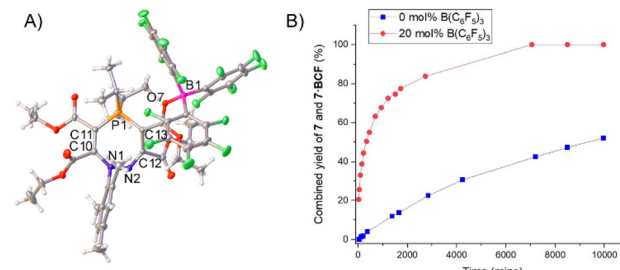


**Fig. 5** (A) Single crystal structure of **7-BCF**. Selected bond distances (Å): P1–C13 1.7791(15), P1–C11 1.7833(16), C12–C13 1.465(2), N2–C12 1.281(2), N1–N2 1.4068(18), O7–B1 1.538(2), N1–C1 1.4571(19), C10–C14 1.530(2), C11–C15 1.471(2), C12–C16 1.533(2), C13–C17 1.383(2), P1–C26 1.8336(16), P1–C29 1.8434(17). Thermal ellipsoids were drawn at the 50% probability level at 120 K.<sup>27</sup> (B) Graph showing conversion of **4** into **7** and **7-BCF** in the absence (blue squares) and presence of 20 mol%  $\text{B}(\text{C}_6\text{F}_5)_3$  in toluene at RT.

subtly different  $^{31}\text{P}\{^1\text{H}\}$  NMR chemical shift to **7** (60.0 ppm (**7-BCF**), 60.4 ppm (**7**)). The fact that the borane is bound to this particular ester group of the four available is consistent with the electron-rich nature of this oxygen centre due to the aforementioned resonance structure  $\gamma$  (Fig. 3E). The bound borane increases the contribution from resonance  $\gamma$  relative to the free **7**; this can be seen in the longer P1–C13 bond distance in **7-BCF** (1.7791(15) Å vs. 1.7465(14) Å in **7**). **7-BCF** could be readily converted to spectroscopically pure **7** by addition of the nucleophilic amine 4-dimethylaminopyridine (DMAP; see ESI, Section S4.3† for details). The same reaction was then monitored with a substoichiometric amount of  $\text{B}(\text{C}_6\text{F}_5)_3$  to assess whether the borane could be used catalytically; the rate of reaction of **4** with one equivalent of  $(\text{C}(\text{CO}_2\text{Et}))_2$  with 20 mol% of  $\text{B}(\text{C}_6\text{F}_5)_3$  was compared to the same reaction without  $\text{B}(\text{C}_6\text{F}_5)_3$  (Fig. 5B).  $\text{B}(\text{C}_6\text{F}_5)_3$  was indeed observed to have a catalytic effect, with the reaction containing 20 mol%  $\text{B}(\text{C}_6\text{F}_5)_3$  reaching 82% conversion in under two days, and full conversion within five days; whereas the reaction without  $\text{B}(\text{C}_6\text{F}_5)_3$  had reached only 21% and 43% conversion at these same timepoints, respectively.

It was established previously that the reaction of the ‘Bu-derivative five-membered ring, **6**, does not react further with the alkyne  $(\text{C}(\text{CO}_2\text{Et}))_2$  to give the seven-membered ring. When this reaction was repeated with the addition of one equivalent of  $\text{B}(\text{C}_6\text{F}_5)_3$ , complete conversion to a new product **11** was evidenced by a new chemical shift in the  $^{31}\text{P}\{^1\text{H}\}$  NMR spectrum

at 85.5 ppm. This chemical shift is significantly more down-field than the  $^{31}\text{P}\{^1\text{H}\}$  NMR shifts for seven-membered rings **7** and **8**. Slow evaporation of an *n*-hexane solution of **11** yielded crystals suitable for SXRD, which revealed that the borane had trapped out the intermediate **I2** from Scheme 5 by binding to the electron-rich carbonyl group in the second equivalent of the alkyne (Scheme 8). Similarly to **4**, the inclusion of  $\text{B}(\text{C}_6\text{F}_5)_3$  presumably lowers the energy barrier to the first step by activating the alkyne to attack from **6**, allowing **11** to form. However, the binding of the borane would also raise the energy of the second step (attack of the nucleophilic carbon to the phosphorus centre) as the carbon is less nucleophilic. In this case with  $\text{R} = {^t\text{Bu}}$  substituents, the energy barrier for the subsequent steps is presumably raised to such an extent that this now become rate-limiting and inaccessible, preventing formation of the analogous seven-membered ring, and stopping the reaction at **11**.

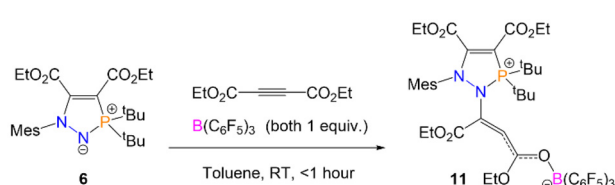
In good agreement with the structure of **I2** (and **11**) predicted by DFT, the single crystal structure of **11** features a partially allenic, partially bent structure, although the bound borane increases the contribution from the allenic structure (Fig. 6). The N2–C26 [1.440(6) Å] and C26–C27 [1.302(6) Å] bond lengths are consistent with an N–C single bond and C=C double bond, while the C27–C28 [1.384(6) Å], being somewhere between single and double bond character.<sup>26,40</sup> The C26–C27–C28 bond angle is 131.9(5) $^\circ$ , consistent with a geometry somewhere between that of an allene and alkene. In

the solution phase, **C27** also possesses a very downfield shift (205.9 ppm) in the  $^{13}\text{C}\{^1\text{H}\}$  NMR spectrum of **11**, in line with other reported allenes.<sup>41,42</sup> DFT and NBO analyses of the structure of **11** (see ESI† for details) is in agreement with the observed crystallographic data. The N2–C26 and C26–C27 bonds possess WBI values of 0.96 and 1.82 respectively, while the WBI for C27–C28 (1.36) is indicative of its partial single- and double-bond character. The HOMO of **11** is located on the lone pair of C27, which resides in an  $\text{sp}^3$  orbital.

**11** can also be viewed as an example of frustrated Lewis pair (FLP) capture of diethyl acetylenedicarboxylate, in which **6** is acting as the Lewis base and  $\text{B}(\text{C}_6\text{F}_5)_3$  acting as the Lewis acid. While capture of alkynes with FLPs is common in the literature, including in FLP-catalysed hydrogenations, non-terminal alkynes predominantly undergo 1,2-addition with FLPs to form an alkene-linked zwitterion.<sup>43</sup> The preference here for 1,4-addition is presumably due to the sterically bulky alkyne, and bulky nitrogen centre on **6** disfavouring 1,2-addition, as well as the ability to form a strong boron–oxygen bond *via* 1,4-addition. The structurally similar alkyne dimethyl acetylenedicarboxylate has indeed been shown to undergo unusual reactivity with FLPs, including 1,4-addition.<sup>44</sup>

## Conclusions

In conclusion, we have described a general route to seven-membered P/N-containing heterocycles *via* azaphosphines. This occurs through initial formation of the corresponding five-membered ring, before P–N bond cleavage yields the analogous seven-membered ring. The stepwise, rather than concerted, nature of these reactions was confirmed by DFT studies, and asymmetric alkynes could be employed for the regioselective synthesis of new heterocycles. The incorporation of  $\text{B}(\text{C}_6\text{F}_5)_3$  revealed both catalytic activity, and allowed for trapping of a reaction intermediate *via* a frustrated Lewis pair-type mechanism. We are continuing to explore the reactivity of the five-membered and seven-membered heterocycles with small molecules for future applications.



**Scheme 8** Reaction of heterocycle **6** with  $(\text{C}(\text{CO}_2\text{Et}))_2$  and  $\text{B}(\text{C}_6\text{F}_5)_3$  to form **11**.

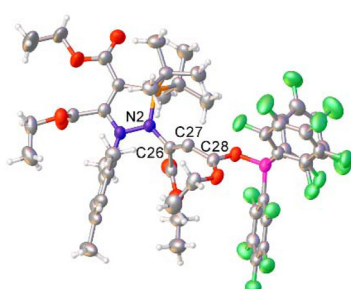


**Fig. 6** Single crystal structure of **11**. Selected bond distances (Å) and angles (°): N2–C26 1.440(6), C26–C27 1.302(6), C27–C28 1.384(6), C26–C27–C28: 131.9(5). **11** crystallised with two product molecules and one hexane molecule in the asymmetric unit; for clarity, only one product molecule is shown here, and the hexane molecule has been omitted. Thermal ellipsoids were drawn at the 50% probability level at 100 K.<sup>27</sup>

## Author contributions

Ethan Calder: investigation, formal analysis, visualisation, writing – original draft preparation. Louise Male: formal analysis (SXRD). Andrew Jupp: conceptualisation, funding acquisition, project administration, resources, supervision, visualisation, writing – reviewing and editing.

## Data Availability

The data associated with this manuscript are available at <https://doi.org/10.25500/edata.bham.00001119>.



## Conflicts of interest

There are no conflicts to declare.

## Acknowledgements

The authors would like to thank the Royal Society (URF\R1\201636), the EPSRC (EP/W036908/1), and the University of Birmingham for funding. The computations described in this paper were performed using the University of Birmingham's BlueBEAR HPC service, see <https://www.birmingham.ac.uk/bear> for more details.

## Notes and references

- 1 F. C. Leavitt, T. A. Manuel and F. Johnson, *J. Am. Chem. Soc.*, 1959, **81**, 3163–3164.
- 2 L. Weber, *Angew. Chem., Int. Ed.*, 2002, **41**, 563–572.
- 3 M. A. Shameem and A. Orthaber, *Chem. – Eur. J.*, 2016, **22**, 10718–10735.
- 4 M. P. Duffy, W. Delaunay, P. A. Bouit and M. Hassler, *Chem. Soc. Rev.*, 2016, **45**, 5296–5310.
- 5 N. Asok, J. R. Gaffen and T. Baumgartner, *Acc. Chem. Res.*, 2023, **56**, 536–547.
- 6 J. A. W. Sklorz and C. Müller, *Eur. J. Inorg. Chem.*, 2016, 595–606.
- 7 J. Bedard and S. S. Chitnis, *Chem. Mater.*, 2023, **35**, 8338–8352.
- 8 J. N. McNeill, J. P. Bard, D. W. Johnson and M. M. Haley, *Chem. Soc. Rev.*, 2023, **52**, 8599–8634.
- 9 S. E. Denmark and T. Wynn, *J. Am. Chem. Soc.*, 2001, **123**, 6199–6200.
- 10 T. Takeda and M. Terada, *J. Am. Chem. Soc.*, 2013, **135**, 15306–15309.
- 11 X. Gao, J. Han and L. Wang, *Org. Lett.*, 2015, **17**, 4596–4599.
- 12 M. L. Helm, M. P. Stewart, R. M. Bullock, M. R. DuBois and D. L. DuBois, *Science*, 2011, **333**, 863–866.
- 13 A. A. Karasik, A. S. Balueva, E. I. Moussina, R. N. Naumov, A. B. Dobrynin, D. B. Krivolapov, I. A. Litvinov and O. G. Sinyashin, *Heteroat. Chem.*, 2008, **19**, 125–132.
- 14 D. M. Weekes, M. G. Jaraquemada-Peláez, T. I. Kostelnik, B. O. Patrick and C. Orvig, *Inorg. Chem.*, 2017, **56**, 10155–10161.
- 15 A.-P. Schaffner, P. Sansilvestri-Morel, N. Despaux, E. Ruano, T. Persigand, A. Rupin, P. Mennecier, M.-O. Vallez, E. Raimbaud, P. Desos and P. Gloanec, *J. Med. Chem.*, 2021, **64**, 3897–3910.
- 16 W. Ried, M. Fulde and J. W. Bats, *Helv. Chim. Acta*, 1990, **73**, 1888–1893.
- 17 S. V. Lozovskiy, A. Y. Ivanov and A. V. Vasilyev, *Beilstein J. Org. Chem.*, 2019, **15**, 1491–1504.
- 18 S. Barkallah, M. Boukraa, H. M'Rabet and H. Zantour, *Synth. Commun.*, 1999, **29**, 1911–1920.
- 19 J. Kroner, W. Schneid, N. Wiberg, B. Wrackmeyer and G. Ziegleder, *J. Chem. Soc., Faraday Trans. 2*, 1978, **74**, 1909–1919.
- 20 N. Wiberg, *Adv. Organomet. Chem.*, 1984, **23**, 131–191.
- 21 O. A. Attanasi, P. Filippone, P. Guerra and F. Serra-Zanetti, *Synth. Commun.*, 1987, **17**, 555–561.
- 22 M. Y. Riu, W. J. Transue, J. M. Rall and C. C. Cummins, *J. Am. Chem. Soc.*, 2021, **143**, 7635–7640.
- 23 K. Tanaka, M. Y. Riu, B. Valladares and C. C. Cummins, *Inorg. Chem.*, 2022, **61**, 13662–13666.
- 24 E. J. Jordan, E. D. E. Calder, H. V. Adcock, L. Male, M. Nieger, J. C. Slootweg and A. R. Jupp, *Chem. – Eur. J.*, 2024, e202401358, DOI: [10.1002/chem.202401358](https://doi.org/10.1002/chem.202401358).
- 25 C. Busacca, T. Bartholomezik, S. Cheekoori, R. Raju, M. Eriksson, S. Kapadia, A. Saha, X. Zeng and C. Senanayake, *Synlett*, 2009, 287–291.
- 26 P. Pykkö and M. Atsumi, *Chem. – Eur. J.*, 2008, **15**, 186–197.
- 27 Deposition numbers 2356186 (4), 2356185 (6), 2356190 (7), 2356192 (7·BCF), 2356188 (8), 2356189 (9), 2356187 (10), and 2356191 (11) contain the supplementary crystallographic data for this paper.†
- 28 A. Schmidpeter and T. von Criegern, *J. Chem. Soc., Chem. Commun.*, 1978, 470–471.
- 29 A. Schmidpeter and T. von Criegern, *Chem. Ber.*, 1978, **111**, 3747–3749.
- 30 W. S. Sheldrick, D. Schomburg, A. Schmidpeter and T. von Criegern, *Chem. Ber.*, 1980, **113**, 55–69.
- 31 Z.-F. Zhang and M.-D. Su, *Dalton Trans.*, 2023, **52**, 4796–4807.
- 32 Y. Chen, S. Ye, L. Jiao, Y. Liang, D. K. Sinha-Mahapatra, J. W. Herndon and Z. X. Yu, *J. Am. Chem. Soc.*, 2007, **129**, 10773–10784.
- 33 J. R. Lawson and R. L. Melen, *Inorg. Chem.*, 2017, **56**, 8627–8643.
- 34 G. C. Welch, R. R. San Juan, J. D. Masuda and D. W. Stephan, *Science*, 2006, **314**, 1124–1126.
- 35 P. A. Chase, G. C. Welch, T. Jurca and D. W. Stephan, *Angew. Chem., Int. Ed.*, 2007, **46**, 8050–8053.
- 36 G. Erker and D. W. Stephan, *Frustrated Lewis Pairs I: Uncovering and Understanding*, Springer, Berlin, Heidelberg, 2013.
- 37 G. Erker and D. W. Stephan, *Frustrated Lewis Pairs II: Expanding the Scope*, Springer, Berlin, Heidelberg, 2013.
- 38 J. C. Slootweg and A. R. Jupp, *Frustrated Lewis Pairs*, Springer, Cham, 2021.
- 39 A. R. Jupp and D. W. Stephan, *Trends Chem.*, 2019, **1**, 35–48.
- 40 P. Pykkö and M. Atsumi, *Chem. – Eur. J.*, 2009, **15**, 12770–12779.
- 41 B. M. Trost, A. B. Pinkerton and M. Seidel, *J. Am. Chem. Soc.*, 2001, **123**, 12466–12476.
- 42 A. S. K. Hashmi, R. Döpp, C. Lothschütz, M. Rudolph, D. Riedel and F. Rominger, *Adv. Synth. Catal.*, 2010, **352**, 1307–1314.
- 43 J. Guo, M. Yan and D. W. Stephan, *Org. Chem. Front.*, 2024, **11**, 2375–2396.
- 44 L. Wang, J. Li, D. Deng, C. G. Daniliuc, C. Mück-Lichtenfeld, G. Kehr and G. Erker, *Dalton Trans.*, 2019, **48**, 11921–11926.

